博士論文

Roles of synaptic activity in climbing fiber to Purkinje cell
synapse elimination in the developing cerebellum

（発達期小脳の登上線維‐プルキンエ細胞シナプスの刈
り込みにおけるシナプス活動の役割）

高　至輝

Roles of synaptic activity in climbing fiber to Purkinje cell synapse elimination
in the developing cerebellum

(発達期小脳の登上線維‐プルキンエ細胞シナプスの刈り込みにおける
シナプス活動の役割)

所属：東京大学大学院医学系研究科機能生物学専攻神経生理学教室

指導教員：狩野方伸

申請者名：高　至輝

ABSTRACT

In postnatal development of vertebrate, mature nerunal circuits are established through refinement of the redundent early-fromed circuits. A key process of the refinement is synapse elimination, in which some of the initially formed synapses are selectively strengthened/maintained and the others are weakened/removed during postnatal development. Studies at the neuromuscular junction (NMJ) or a few regions in the central nervous system (CNS) collectively suggest that "winner" synapses to be strengthened/maintained are discriminated from "loser" synapses to be weakened/removed depending on synaptic activity. However, it remains unknown to what extent competition among synaptic inputs contributes to the whole processes of developmental synapse elimination. It remains also to be elucidated whether the common mechanisms underlie developmental synapse elimination at different regions of the CNS. Here, I tackled these problems in climbing fiber to Purkinje cell synapse in the developing cerebellum, which is one of the best studied model for synapse elimination. I established methods that abolish neurotransmitter release from a subset of climbing fibers almost throughout the entire period of postnatal development by *in vivo* lentiviral–mediated infection of tetanus-toxin light chain (TNLC) into climbing fibers. With this new technique, I discovered unexpected evidence that the selection of "winners" and "losers" is not dependent on climbing fiber to Purkinje cell synaptic strength. However, synaptic activity is required for proper extension of innervation by a single "winner" climbing fiber over Purkinje cell dendrites. Furthermore, synaptic activity is essential for eliminating redundant "loser" climbing fiber synapses from the soma of Purkinje cells. These new findings clarified the roles of synaptic activity in the processes of developmental synapse elimination and gives a new insight into the mechanisms of neural circuit refinement in the developing nervous system.

CONTENTS

INTRODUCTION

In both central and peripheral nervous systems of the vertebrates, early formed synaptic connections are usually redundant and require refinement through a series of developmental processes, known as synapse elimination, to transform the initially formed immature neural circuits into their functionally mature versions (Lichtman and Colman, 2000; Kano and Hashimoto, 2009; Watanabe and Kano, 2011). One of the classical examples for synapse elimination is the refinement of developing neuromuscular junctions (NMJs) in the peripheral nervous system. At birth, each muscle fiber receives projections from multiple motor neurons. Then all but one motor neuron axons are subsequently removed during postnatal development (Purves and Lichtman, 1980). A further study at developing NMJs revealed a divergence of synaptic strength between two motor neuron axons projecting to the same muscle fiber during the refinement. The authors demonstrated that axons with higher synaptic strengths were further strengthened, while those with lower synaptic strengths were progressively weakened and eventually removed from the muscle fibers within a 1-2 days period after the divergence became obvious (Colman et al., 1997). Importantly, another study at mouse NMJs in which choline acetyltransferase (ChAT) was deleted in a part of motor neurons demonstrated that ChAT deleted motor axons with weaker synaptic inputs always had less occupancy in the competition with ChAT expressing motor axons (Buffelli et al., 2003). Moreover, the same group found that the laser ablation of the winning axon resulted in a gradual takeover of the vacated postsynaptic spaces on the corresponding muscle fiber by the soon-to-be eliminated motor axon (Turney and Lichtman, 2012). Collectively, these lines of evidence strongly suggest that synapse elimination, at least at developing NMJs, is mediated by competition between the co-projecting motor axons in a highly dynamic manner, and the outcome of the

competition is determined by relative difference in synaptic strength between the competing motor axons.

Several forms of synapse elimination with similar mechanisms to those at the NMJs have been found in the central nervous system. A classical example is ocular dominance plasticity in the developing visual cortex. Neurons in the immature visual cortex normally respond to stimuli presented to both eyes, and then they come to respond preferentially to one of the eyes after maturation (Wiesel and Hubel, 1963). It has been shown that deprivation of one eye during a period of postnatal development, known as critical period or sensitive period, causes a shift of neuronal spiking response and innervation territories of geniculo-cortical afferents in favor of the open eye (Wiesel and Hubel, 1963; Hubel and Wiesel, 1970; 1977). Similarly, synapse elimination at the developing retinogeniculate projection is reported to involve activity-dependent competitive processes. Projections from retinal ganglion cells of each eye are intermingled in the lateral geniculate nucleus at the early developmental stage, but they are subsequently segregated into each specific area of the lateral geniculate nucleus (Linden et al., 1981; Shatz, 1983; Godement et al., 1984; Sretavan and Shatz, 1986). Deprivation and increase of sensory inputs from one eye cause the decrease and the expansion, respectively, of the territories innervated by the retinal ganglion axons corresponding to that eye (Stellwagen and Shatz, 2002; Hayakawa and Kawasaki, 2010). Moreover, the rearrangement was impaired by synchronous stimulation of retinal ganglion cells in both eyes (Zhang et al., 2011). These findings suggest that the strength and the timing of neural activity including synaptic inputs are crucial for the rearrangement.

For the third example, projections in several sub-regions of the developing hippocampus are reported to be reorganized based on activity-dependent competition

between the excitatory inputs. Remarkably, inactive inputs that are incapable of releasing glutamate are all subsequently replaced by active inputs during postnatal development of the hippocampus (Yasuda et al., 2011). Importantly, this rearrangement does not occur when the activities of all the inputs and postsynaptic neurons in a sub-region of the hippocampus are blocked by TTX, indicating that synaptic inputs which can activate postsynaptic neurons will win and replace those which cannot activate postsynaptic neurons (Yasuda et al., 2011).

However, it remains unknown to what extent competition among synaptic inputs contributes to the whole processes of developmental synapse elimination. This is presumably because of the difficulty to block synaptic transmission completely in only a part of presynaptic neurons during the entire course of postnatal neural circuit refinement. It remains also to be elucidated whether common mechanisms underlie developmental synapse elimination at different regions of the central nervous system (CNS). Another limitation of the aforementioned examples of developmental synapse elimination in the CNS is the complexity in neuronal connectivity. In this respect, elimination of redundant climbing fiber to Purkinje cell synapses during postnatal development of the cerebellum provides a good model of developmental synapse elimination in the CNS.

Each Purkinje cells is initially innervated by multiple climbing fibers with similar synaptic strengths around birth (Crepel et al., 1976). A single climbing fiber is selectively strengthened in each Purkinje cell from postnatal day 3 (P3) to P7 (Hashimoto and Kano, 2003). Then, from P9, only the strengthened climbing fiber (the "winner" climbing fiber) translocates along growing Purkinje cell dendrites and forms synapses there, whereas the other weaker climbing fibers ("loser" climbing fibers) stay on the somata (Hashimoto et al., 2009) and are subsequently eliminated from the somata

from P7 to around P11 ("early phase" of climbing fiber elimination) and from around P12 to P17 ("late phase" of climbing fiber elimination) (Hashimoto et al., 2009). Two studies demonstrated that long-term potentiation (LTP) can be induced at synapses from strong climbing fibers while the same stimulation protocol induces long-term depression (LTD) at synapses from weak climbing fibers in acute cerebellar slices (Bosman et al., 2008; Ohtsuki and Hirano, 2008). Hashimoto et al. (2011) demonstrated that selective strengthening of a single climbing fiber and its dendritic translocation in each Purkinje cell requires Ca^{2+} influx into Purkinje cells through P/Q-type voltage-dependent Ca^{2+} channels (Hashimoto et al., 2011). Results from *in vivo* electrophysiological experiments in rats during postnatal cerebellar development suggested that single climbing fiber inputs may be strengthened in individual Purkinje cells in a spike timing-dependent manner (Kawamura et al., 2013). These studies in the cerebellum of young rodents are consistent with the notion that a single winner climbing fiber is selected in each Purkinje cell synapse by activity-dependent competition among multiple climbing fibers innervating the same Purkinje cell. The competitive feature of climbing fibers co-projecting to the same Purkinje cell was proven by a time-lapse imaging study that laser ablation of the already translocated "winner" climbing fiber results in translocation of another "loser" climbing fiber (Carrillo et al., 2013). The same time-lapse study showed that most of the climbing fibers occupying the widest territories on the soma subsequently translocate to dendrites to become "winners". However, the same study also found that a minor portion of climbing fibers with predominant territory on the soma did not become the subsequent "winners" (Carrillo et al., 2013), which apparently is at variance with the hypothesis of activity-dependent selection of winner climbing fibers. This data prompted me to further investigate the roles of synaptic inputs in the selection of winner climbing fibers,

since climbing fibers innervating more territory induce stronger synaptic responses in corresponding Purkinje cells (Carrillo et al., 2013).

To interrogate to what extent synaptic activity is crucial for the determination of single "winner" climbing fibers in individual Purkinje cells, I tried to establish an experimental system in which neurotransmitter release from a subset of climbing fibers is abolished during early postnatal development. I used lentiviral infection of vectors carrying microRNA targeting SNAP25 or those for expression of tetanus toxin light-chain (TNLC) to neurons in the inferior olive, the origin of climbing fibers. SNAP25 is a member of presynaptic SNARE machinery, which plays crucial roles in stimuli-dependent neurotransmission (Washbourne et al., 2002). TNLC is a truncated version of tetanus toxin and known to completely deplete presynaptic release through specific proteolysis of synaptic VAMP2 (Schiavo et al., 1992). Therefore, both knockdown of SNAP25 and expression of TNSC in inferior olivary neurons are expected to interrupt/terminate neurotransmitter release from climbing fiber synaptic terminals. I examined the fate of climbing fibers that are not capable of releasing glutamate ("absolutely weaker" climbing fibers) during postnatal development and in adulthood. The results are rather unexpected. I found that "absolutely weaker" climbing fibers sometimes became ultimate "winner" climbing fibers. This result suggests that the selection of a single "winner" climbing fiber in each Purkinje cell is not dependent on the strength of synaptic activity. However, extension of "absolutely weaker" climbing fiber along Purkinje cell dendrites was incomplete, and that somatic climbing fiber synapses were not eliminated in Purkinje cells that had single "absolutely weaker" climbing fibers on the dendrites. These results indicate that climbing fiber synaptic activity is crucial for proper extension of climbing fiber innervation territory and elimination of redundant climbing fiber synapses on the soma.

MATERIALS AND METOHDS

Animals

C57BL/6N mice (SLC JAPAN) or transgenic mice expressing enhanced green fluorescent protein (EGFP) under the control of neurofilament light-chain (nefl) promoter (nefl-EGFP; Mutant Mouse Regional Resource Centers, 015882-UCD) were used for this study. The same nefl-EGFP mouse line I used in this study were previously demonstrated by Carrillo et al. that those mice express EGFP in a subset of their climbing fibers since early postnatal days (Carrillo et al., 2013). All procedures for animal care and experiments were made in accordance with the guidelines of the institutional animal care and use committee (IACUC) of the University of Tokyo, and approved by the IACUC .

Virus vector construction

Lentiviral vectors designed to express SNAP25 (NCBI: NM_011428.3), miRNA-resistant SNAP25, fluorescent marker (EGFP or mOrange2), TNLC (NCBI: AAC37720; with further codon optimization for mouse expression), and TNLC-P2A-EGFP (TNLC gene followed by EGFP connected with a self-cleaving P2A linker) were modified from the previously described murine embryonic stem cell virus (MSCV) driven VSV-G pseudotyped lentiviral vectors (pCL20c-MSCV) (Uesaka et al., 2014). The cDNA of SNAP25 gene were obtained by RT-PCR from P10 mouse medulla. The SNAP25 gene with it's 5'UTR was amplified from the cDNA and subcloned into the lentiviral vector, and the same mouse SNAP25 gene except it's 5'UTR region was cloned into the same expression vector to express miRNA-resistant SNAP25 (Res-SNAP25). The BLOCK-iT Pol II miR RNAi expression vector kit (Invitrogen, CA, USA) was used for vector-based RNA interference (RNAi) experiment.

The following engineered microRNA was designed according to the BLOCK-iT Pol II miR RNAi Expression Vector kit guidelines (Invitrogen) for targeting mouse SNAP25 gene at 5'UTR region or open reading frame by the following pairs of oligonucleotides, respectively:

5'-TGCTGTAAAGAACCTTGTCTTCTCCGGTTTTGGCCACTGACTGACCGGAG AAGAAGGTTCTTTA-3' and

5'-CCTGTAAAGAACCTTCTTCTCCGGTCAGTCAGTGGCCAAAACCGGAGAAG ACAAGGTTCTTTAC-3' pair was designed for targeting 5'UTR of SNAP25 mRNA.

5'-TGCTGTCCTGATGCCAGCATCTTTACGTTTTGGCCACTGACTGACGTAAAG ATTGGCATCAGGA -3' and

5'-CCTGTCCTGATGCCAATCTTTACGTCAGTCAGTGGCCAAAACGTAAAGAT GCTGGCATCAGGAC -3' pair was designed for targeting the open reading frame region of SNAP25 mRNA.

Those oligonucleotides were subcloned into a pCL20c-MSCV vector described above to generate SNAP25 targeting miRNA lentiviral vector. The one designed for targeting the open reading frame region of SNAP25 mRNA were proved to have no knockdown effect toward mouse SNAP25 and were subsequently used as control miRNA.

Virus production

Lentiviral particles were produced by the previously described method (Mikuni et al., 2013; Kawata et al., 2014; Uesaka et al., 2014). Briefly, a vector containing one of the desired genes (miSNAP25, Res-SNAP25, EGFP, mOrange2, TNLC-P2A-EGFP or TNLC) was co-transfected with packaging plasmids (psPAX2 and pCAG-VSVG) into human embryonic kidney (HEK) 293T cell line via a calcium phosphate precipitation

method. After 40 hours, viral particles were collected via ultracentrifugation (120,000 x g, 90 minutes), and suspended in 35 μL PBS, and the final products were stocked in 4°C. Expiring day of each viral solution was set to 14 days after it was harvested.

Evaluation of SNAP25 knockdown efficiency in HEK293T

The lentiviral vectors were introduced into HEK293T cell line using Lipofectamine® LTX with Plus™ Reagent (Thermo Fisher Scientific Inc.). 0.25 mg of miSNAP25 or Control miRNA were mixed with 0.25 mg of SNAP25 or Res-SNAP25 in the mixtures containing 0.5 μL of PLUS™ reagent, 1uL of Lipofectamine® LTX reagent, and 25 μL of Opti-MEM (Thermo Fisher Scientific Inc.). After incubation in room temperature for 30 minutes, transfections were conducted by introducing the mixtures to 10-30% confluent HEK293T cells in 24-well culture plate. The transfected cells were incubated at 37°C in a 5% CO_2 in air atmosphere for 24 hours. Medium changes were carried out 8 hours after transfections, and the cells were incubated for another 24 hours. Then, cells in each well were washed by PBS twice and fixed with 4% paraformaldehyde for 10 minutes (Nacalai TESQUE, inc.). The fixed HEK293T cells were washed for 10 minutes with PBS 3 times, and blocking with donkey serum for 40 minutes. Primary antibodies recognizing mouse SNAP25 (mouse IgG; Synaptic Systems Inc.) or EGFP (rat IgG; Nacalai TESQUE, inc.) were introduced to the transfected cells and the cells were incubate overnight at 4°C. After washed with PBS, cells were incubated with cy3 and Alexa488 conjugated secondary antibodies recognizing mouse and rat IgG, respectively, for 3 hours, and washed with PBS. Images of 10 randomly picked regions of interest (ROIs) were collected from cells transfected with each lentiviral vector pairs by confocal microscopy (FV1200, Olympus). The total SNAP25 (I_{SNAP25}) and EGFP (I_{EGFP}) signal intensities were measured with ImageJ, and

normalized SNAP25 intensities for each ROIs were calculated by I_{SNAP25}/ I_{EGFP}. Normalized SNAP25 intensities from 10 ROIs were averaged to generate the final results for each condition.

Virus infection

Similar to the protocol described in the previous study (Uesaka et al., 2014), lentiviral particles were injected into ventral medial portion of the medulla of C57BL/6N (WT) or nefl-EGFP mice. For lentiviral mixture microinjection, mice were anesthetized with isoflurane. For usual *in vivo* virus infection into the inferior olivary neurons, 0.8–1.5 μL (0.8–1.5×10^5 TU) of viral solution was injected at P1.

For *in vivo* virus infection of TNLC into inferior olivary neurons, I tried TNLC-P2A-EGFP lentiviral vector for expression of both TNLC and EGFP. I found that the infection via this lentiviral vector was lethal to most mice when 0.3–0.8 μL (0.3–0.8×10^5 TU) of viral solution was injected. This lethal effect could be avoided by a 1:4 dilution of the viral solution by PBS. However, the expression of the fluorescent marker on early postnatal days was not sufficient for electrophysiological experiments. For these reasons, I harvested a mixture of lentiviral vectors for expression of TNLC and fluorescent marker (EGFP or mOrange2) separately at the same day. Each P1 pups or P16 mice were infected with 0.4 - 0.8 μL or 1.5 μL of viral mixture into their ventral medial portion of the medulla. The final viral solutions were optimized to the TNLC to fluorescent marker ratio of 1:4. This viral mixture was not lethal for most of the infected mice and provided visible climbing fibers for our electrophysiological survey at least 4 days after injections.

Electrophysiology

For electrophysiological experiments, infected mice at the age between P5 and P26 were anesthetized with carbon dioxide and sacrificed by decapitation. Parasagittal cerebellar slices (250 μm) were prepared as described previously (Aiba et al., 1994). The slices were then bathed in a reservoir chamber in a solution composed of 125 mM NaCl, 2.5 mM KCl, 2 mM $CaCl_2$, 1 mM $MgSO_4$, 1.25 mM NaH_2PO_4, 26 mM $NaHCO_3$, and 20 mM glucose, which was bubbled with 95% O_2 and 5% CO_2 for further 1 hour before being transferred to the experiment stage of an Olympus BX51WI microscope. Oxygen was continuously provided to the stage by perfusing oxygenated bath solution that contained picrotoxin (TOCRIS; 0.1 mM) to block $GABA_A$ receptor-mediated inhibitory synaptic transmission. Temperature of the chamber in all experiments was held at 32°C. Patch pipettes were filled with an intracellular solution composed of 60 mM CsCl, 10 mM Cs D-gluconate, 20 mM TEA-Cl, 20 mM BAPTA, 4 mM $MgCl_2$, 4 mM ATP, and 30 mM HEPES (pH 7.3, adjusted with CsOH). Resistance of patch pipettes was usually between 1.5–2.5 MΩ and the pipette access resistance was compensated by 70%. In most cases, Alexa 568 (final concentration: 100 μM, Life Technologies) was added to the internal solution for locating the recorded Purkinje cells. In each recording, a total diffusion time for Alexa 568 was 10-15 minutes or more after achieving whole-cell configuration to assure sufficient diffusion of the fluorescent dye into the dendrites of Purkinje cells. Climbing fiber-mediated excitatory postsynaptic currents (CF-EPSCs) were elicited at the holding potential of -10 mV or -70 mV (corrected for the liquid junction potential) by electrical pulse stimuli (duration, 0.1 ms) at 0.2 Hz applied to the granule cell layer 20–100 μm from the targeted Purkinje cell soma. To search all the climbing fibers innervating the Purkinje cell under recording, stimulation was applied at up to 10 different locations and the stimulus current intensity was gradually increased from 0 to 30 μA at each location. If no CF-EPSCs were elicited

even with the systematic survey (showing no signal larger than baseline noise without stimulation; signal < $mean_{noise} \pm 2$ s.d. $_{noise}$), the total amplitude of CF-EPSCs to that Purkinje cell was judged to be 0 ($EPSC_{total}=0$). When the fluorescence from climbing fibers could not be confidentially detected under the fluorescent microscope during electrophysiological recording, the slices were transferred to the confocal laser scanning microscope (FV1200, Olympus) for further evaluation. Purkinje cells that could not be clearly classified whether they were accessed by fluorescent-positive or –negative climbing fibers were excluded from the data.

Immunohistochemistory

Under deep pentobarbital anesthesia (100 μg/g of body weight, intraperitoneal injection), mice were perfused with 4% paraformaldehyde in 0.1 M phosphate buffer and processed to obtain parasagittal sections (80-100 μm in thickness). After permeabilization and blockage, slices were incubated with primary antibodies. Several combinations of primary and secondary antibodies were assigned for 3 channel or 4 channel confocal imaging of the sections. Primary antibody recognizing Car8 (guinea pig, goat, or rabbit IgG; Frontier institute co., ltd.), a molecular marker representing Purkinje cells, vGluT2 (rabbit, guinea pig or goat IgG; Frontier institute co., ltd), a molecular marker representing climbing fiber to Purkinje cell synapses, EGFP (Rat IgG; Nacalai TESQUE, inc.) and mOrange2 (Rabbit IgG; Clontech laboratories inc.) were selectively incubated with parasagittal sections at 4°C overnight. Than, combinations of secondary antibodies conjugated to Delight 405 (recognizing guinea pig IgG; The Jackson Laboratory), Alexa 488 (recognize Rat IgG; The Jackson Laboratory), cy3 (recognize rabbit or guinea pig IgG; The Jackson Laboratory), or Alexa 647 (recognizing guinea pig, goat, or rabbit IgG; The Jackson Laboratory) were selected

according to the prior assigned primary antibodies to incubate with the washed parasagittal sections for 3 further hours at room temperature. Those immunolabeled sections were then washed and mounted for observations with the confocal laser scanning microscope (FV1200, Olympus).

Data Analysis

Analysis of climbing fiber height

Z-stacked images collected from the immunolabeled cerebellar sections of TNLC+mOrange2 infected nefl-EGFP adult mice (>P20) were used in this analysis. The height of climbing fibers was determined as previous studies (Kawata et al., 2014). In brief, I measured the distances between the vGluT2 signal at the tip of dendrite and the top of the soma (the "neck") of Purkinje cells as a raw climbing fiber height with the measure function of ImageJ. The relative climbing fiber height was calculated by dividing this raw climbing fiber height by the thickness of the corresponding molecular cell layer.

Morphological analysis for the determination of a "winner" climbing fiber

Z-stacked images collected from the immunolabeled parasagittal cerebellar sections from EGFP or TNLC+EGFP infected WT mice at P12 or P15, respectively. In this analysis, I sampled only the Purkinje cells that fulfilled the following criteria: 1. Purkinje cells unambiguously innervated by single "winner" climbing fibers on their dendrites. 2. Purkinje cells innervated by both infected and non-infected climbing fibers. Purkinje cells innervated by infected wining climbing fibers and those by uninfected winner climbing fibers were classified as the "winner" group and the "loser"

group, respectively. I used the 3D view function of ImageJ for further evaluation. Samples that cannot be unequivocally categorized were excluded.

Morphological analysis of multiple climbing fiber innervation

Z-stacked images collected from the immunolabeled parasagittal cerebellar sections of infected nefl-EGFP mice were used in this analysis. I collected Purkinje cells innervated by single winning infected climbing fibers as many as possible, and categorized them into mono-innervated and multiply-innervated groups similar to the previous studies (Miyazaki and Watanabe, 2010; Mikuni et al., 2013; Kawata et al., 2014). In brief, I searched for vGluT2-positive puncta that did not overlap with the fluorescent marker of infected climbing fibers on the soma of each Purkinje cell innervated by a winning infected climbing fiber on its dendrites. Purkinje cells with such vGluT2-positive puncta on their somata were classified into the "mutliply-innervated" group, and those with no such vGluT2-positive puncta were into "mono-innovated" group. I used the 3D view function of ImageJ for further evaluation. Samples that cannot be unequivocally categorized were excluded.

RESULTS

Strategy to test roles of synaptic activity in climbing fiber synapse elimination

To examine the roles of synaptic activity in climbing fibers to Purkinje cell synapse elimination, I deprived glutamate release from a subset of climbing fibers by infections of lentiviral vectors carrying RNAi knockdown sequences against SNAP25 or those for the expression of tetanus toxin to a part of inferior olivary neurons, the origins of climbing fibers. I chose this strategy rather than the direct manipulation of activities of inferior olivary neurons because the latter procedure may also change the firing of non-infected inferior olivary neurons through electrical coupling with adjacent infected neurons via gap junctions (Sotelo et al., 1974).

Reduced synaptic inputs from miSNAP25 infected climbing fibers

To reduce synaptic inputs to Purkinje cells from a subset of climbing fibers, I selected SNAP25 as the target of knockdown because SNAP25 is a member of presynaptic SNARE complex and plays crucial roles in stimuli-dependent neurotransmission. A previous study demonstrates that SNAP25 knockout mice show the complete lack of stimuli-dependent neurotransmission at neuromuscular junctions and in hippocampal neurons (Washbourne et al., 2002). For knockdown of SNAP25, in mice, I constructed a lentiviral microRNA (miRNA) vector targeting SNAP25 (miSNAP25, Fig.1a), I also constructed lentiviral vectors for expression of SNAP25 (SNAP25) and miSNAP25-resistant SNAP25 (res-SNAP25) (Fig. 1a, see material methods) (Uesaka et al., 2014). First I checked the knockdown efficacy and specificity of miSNAP25 in HEK293T cell line (see materials and methods). I examined expression levels of SNAP25 by transfecting the SNAP25 or Res-SNAP25 lentiviral vector with the miSNAP25 or control miRNA lentiviral vector that had no expected

knockdown effects (Ctrl-miRNA, a malfunctioning miRNA vector; see materials and methods). I found that the miSNAP25 induced a significant suppression on SNAP25 expression driven by the lentiviral vector containing mouse SNAP25 gene (miSNAP25+SNAP25, 0.379± 0.021; the second panel in Fig.1b) compared to that conducted with the Ctrl-miRNA vector (Ctrl-miRNA+SNAP25, 0.619±0.019; 2; the first panel in Fig.1b). The co-transfection of the Res-SNAP25 vector with the miSNAP25 vector effectively rescued the expression of SNAP25 (miSNAP25+ Res-SNAP25, 0.689±0.05; the third panel in Fig. 1b) with no significant difference compared to the expression level of SNAP25 after co-transfection with the control miRNA vector (Ctrl-miRNA+ Res-SNAP25, 0.737±0.045; the fourth panel in Fig. 1b). These results indicate that this lentiviral miSNAP25 vector can be utilized for knockdown of mouse SNAP25, and the expression of SNAP25 can be rescued by the Res-SNAP25 lentiviral vector. Therefore, these vectors are suitable for the following experiments to deplete a subset of climbing fiber synaptic inputs to Purkinje cells.
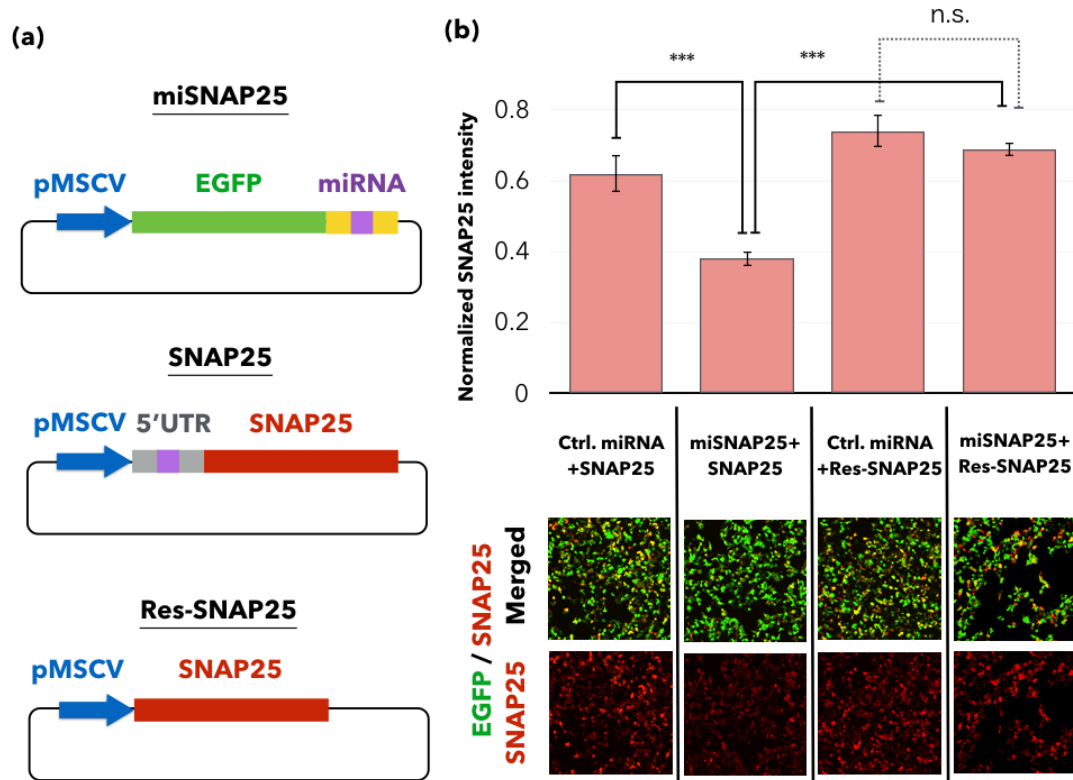
Figure 1. Efficacy and specificity of knockdown of mouse SNAP25 by a miSNAP25 lentiviral vector.

a. Cartoons representing the design of three lentiviral vectors modified from the pCL20c-MSCV vector. Colored arrows and rectangles represent sequences as described below: blue arrow: MSCV promoter; green rectangle: EGFP; yellow rectangle: universal sequence designed for miRNA cloning; magenta rectangle within the yellow rectangle: designed miRNA sequence; gray rectangle: 5'UTR of intrinsic mouse SNAP25, magenta rectangle within the gray rectangle: sequence targeted by the designed miRNA; red rectangle: mouse SNAP25. b. Evaluation of knockdown efficiency of the miSNAP25 vector using HEK293T. Experimental conditions are indicated in the middle row. The upper bar graph indicates the normalized fluorescent intensities representing the expression level of SNAP25. The lower images are examples ROIs for the corresponding groups under confocal microscopy. *** $p < 0.001$, n.s. $p > 0.05$ (t- test). Error bars stand for ± SEM.
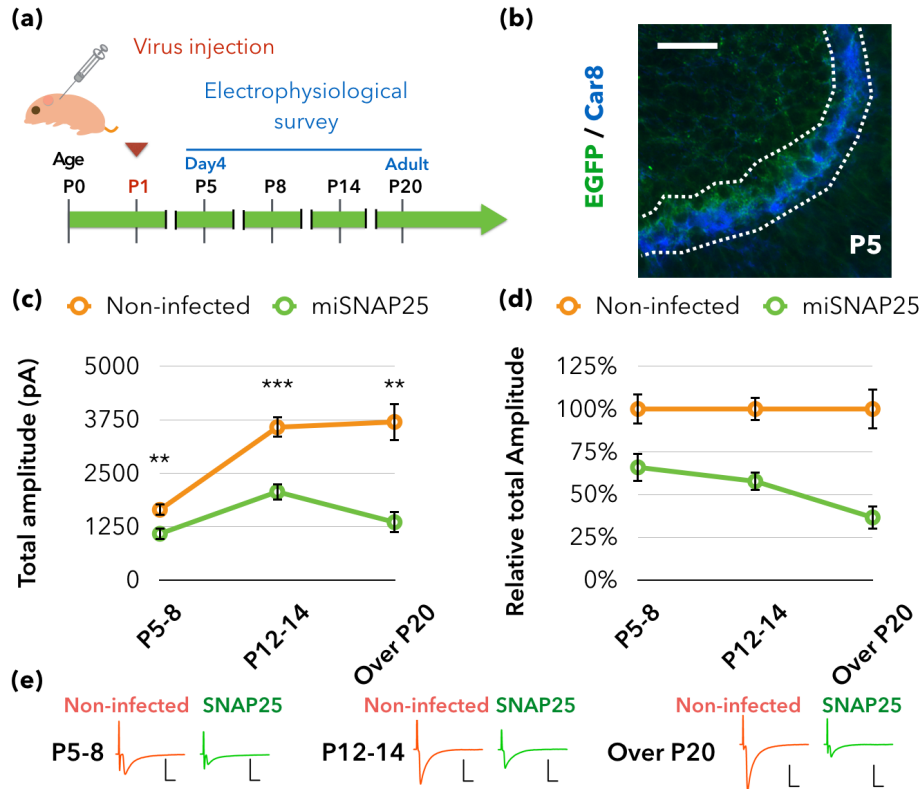
I infected the inferior olivary neurons of the wild-type mouse pups at postnatal day (P) 1 with the miSNAP25 lentiviral vector (Fig.1a) (WT, see materials and methods). Then I evaluated the effect of SNAP25 knockdown on climbing fiber synaptic inputs in different developmental stages by using the electrophysiological method (Fig. 2a, see materials and methods). I performed whole-cell patch-clamp recording from Purkinje cells in acute cerebellar slices, and recorded excitatory postsynaptic currents (EPSCs) induced by stimulating climbing fibers in the granule cell layer. In the infected mice, Purkinje cells innervated by EGFP-positive climbing fibers were assigned to the miSNAP25 group (Fig. 2b) and those innervated by EGFP-negative climbing fibers were assigned to the control group. I found that the average total EPSC amplitude of the miSNAP25 group reduced from that of the control group by 34% in the first postnatal week (P5-8; miSNAP25: 1083.21 ± 141.59 pA, n=76; control: 1643.66 ± 148.7 pA, n=82; Fig. 2c,d; p<0.01), by 42% in the second postnatal week (P12-14; miSNAP25: 2063.81 ± 201.7 pA, n= 41; control: 3574.28 ± 249.97 pA, n= 42 Fig. 2c,d; p<0.001), and by 63% in adulthood (over P20; miSNAP25: 1353.4 ± 257.95 pA, n= 7; control: 3697.57 ± 446.38 pA, n= 16; Fig 2c, d; p<0.01). Thus, the infection of the lentiviral miSNAP25 vector to inferior olivary neurons caused a significant suppression of climbing fiber to Purkinje cell synaptic transmission.

**Decreased dendritic translocation of miSNAP25 infected climbing fibers**

I next examined the morphology of the miSNAP25 infected climbing fibers in young adult mice. A previous study suggests that decreased synaptic inputs to Purkinje cells cause impairment in translocation of climbing fibers onto Purkinje cell dendrites (Kawata et al., 2014). The fact that a similar phenotype is observed in knockout mice deficient in P/Q-type voltage-dependent Ca^{2+} channel further suggests that synaptic inputs from climbing fibers mediates dendritic translocation because this channel is thought to be activated mainly by climbing fiber synaptic inputs (Hashimoto et al., 2011). I examined the extent of climbing fiber translocation by analyzing the height of climbing fibers relative to the thickness of the molecular layer. I measured the distance between the top of the Purkinje cell soma and the most distal signal of vesicular glutamate transporter type 2 (VGluT2), a climbing fiber terminal marker. This value was divided by the height of the thickness of the corresponding region of the molecular layer (see materials and methods). miSNAP25 infected climbing fibers showed significant reduction in their heights compared to non-infected control climbing fibers in the same sections (miSNAP: $51 \pm 2\%$, n= 39; control: $69 \pm 2\%$, n= 32; Fig 3c; $p< 0.001$). The reduced climbing fiber translocation by the miSNAP25 was successfully rescued when the Res-SNAP25 (Fig 1a) was co-infected with the miSNAP25 (miSNAP+Res-SNAP25: $66\pm3\%$, n=10; control: $66\pm3\%$, n=10; Fig 3c; $p>0.05$). Taken together, consistent with previous studies (Kawata et al., 2014), these results indicate that climbing fiber to Purkinje cell synaptic transmission plays an important role in the proper translocation of climbing fibers to Purkinje cell dendrites during postnatal development. However, since the blockade of climbing fiber to Purkinje cell transmission by the SNAP25 knockdown was incomplete, I could not estimate precisely

to what extent climbing fiber synaptic activity contributes to the winner-loser discrimination.

Figure 2. Suppression of climbing fiber to Purkinje cell synaptic transmission after transfection of the miSNAP25 into inferior olivary neurons

a. Experimental schedule. The inverted triangle indicates the time of viral injection. b. Example of cerebellar slice used for electrophysiological recording, and then fixed and stained thereafter. The area between two white dotted lines indicates the somata of Purkinje cells. green, EGFP; blue, car8. The scale bar represents 30 μm. c. Line-chart representing the average total amplitudes of EPSCs elicited by stimuli on climbing fibers in control (orange) and miSNAP25 (green) Purkinje cells. d. Relative total amplitudes of CF-induced EPSCs from the same experiments in (c). e. Example traces of each group in (c). The vertical and horizontal scale bars represent 2 nA and 5 ms, respectively. Total EPSC amplitudes of miSNAP25 Purkinje cells are normalized by those of control Purkinje cells at corresponding ages. ** $p < 0.01$, *** $p < 0.001$, n.s. $p > 0.05$ (Wilcoxon–Mann–Whitney test). Error bars stand for ±SEM.
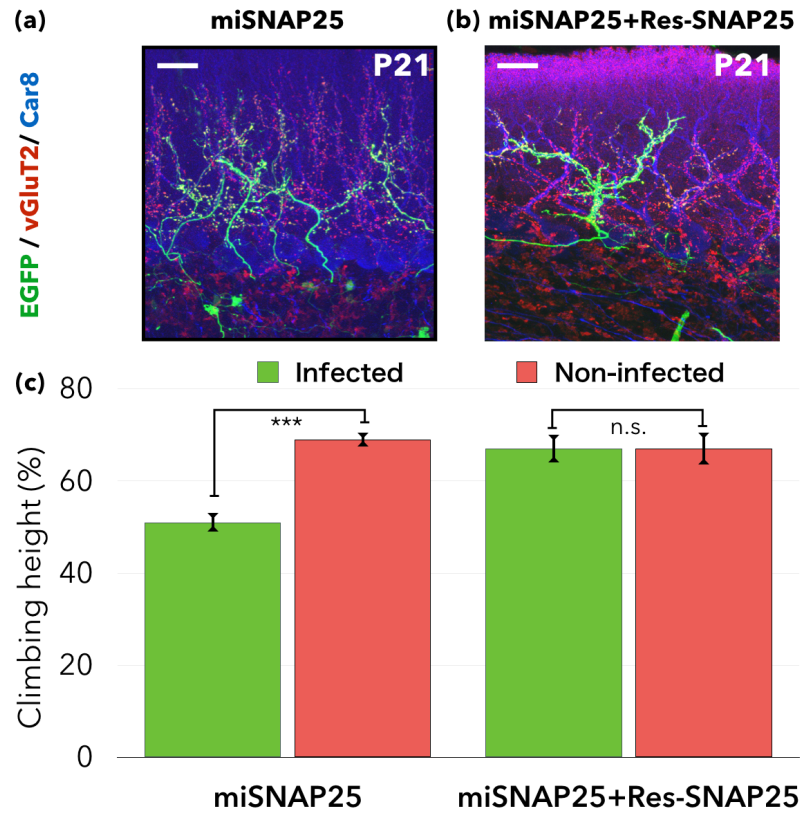
**Figure 3. Decreased heights in miSNAP25 infected climbing fibers in adulthood.**

a,b. Example confocal images for climbing fibers infected with miSNAP25 (a) and with miSNAP25 plus Res-SNAP25 (b). green, EGFP; red, vGluT2; blue, Car8. The scale bars represent 30 μm. c. Bar graphs showing the climbing fiber height relative to the molecular layer thickness for mice infected with miSNAP25 (left) and with miSNAP25 plus Res-SNAP25 (right). Green and red columns represent the relative heights of infected and non-infected control climbing fibers, respectively, from the same cerebellar sections. *** $p < 0.001$, n.s. $p > 0.05$ (t-test). Error bars stand for ± SEM.

Ablation of climbing fiber to Purkinje cell synapse inputs by TNLC

I next tried to achieve a complete ablation of glutamate release from climbing fibers by expressing tetanus toxin light-chain (TNLC) into inferior olivary neurons. TNLC is a truncated version of tetanus toxin, an extremely potent neurotoxin produced by the vegetative cell of *Clostridium tetani*. This shortened version of toxin contains the protease domains (Blasi et al., 1993), and has been previously proved to completely deplete neurotransmitter release through specific proteolysis of synaptic VAMP2 (also known as synaptobrevin 2) *in vivo* (Kerschensteiner et al., 2009; Yasuda et al., 2011). I subcloned the TNLC gene into the lentiviral vector expressing a fusion protein composed of TNLC, EGFP and a self-cleaving P2A peptide between these two proteins (TNLC-P2A-EGFP) (Fig. 4). Then I infected this lentiviral TNLC-P2A-EGFP vector into inferior olivary neurons of mice at P1. I found that the infection of this viral vector with high titer resulted in lethality of the infected pups. Although the survival rates was improved by the dilution of the vial solution, the fluorescent intensity by EGFP was not sufficient to unequivocally identify infected climbing fibers in electrophysiological experiments of early postnatal mice (P5-8, also see materials and methods).

To reduce the lethal effect by TNLC and to maintain the strong fluorescent signals, I used a mixture of two lentiviral vectors, one for TNLC expression and the other for EGFP expression (Fig. 4). To examine the expression pattern of each gene in the cerebellum, I first infected a mixture of each lentiviral vector with EGFP or mOrange2 which were mixed in 1:1 ratio to the inferior olivary neurons at P1 (see materials and methods). This method resulted in sufficient labeling of climbing fibers with a highly-overlapped expression pattern for EGFP and mOrange2 (Fig. 5b). I also observed essentially the same highly-overlapped expression in mice infected at P1, with

viral mixture being the EGFP:mOrange2 ratio of 4:1. I found that 87.3% of climbing

fibers contained both EGFP and mOrange2 at P15 (Fig. 5c, yellow block; total n=237

climbing fibers from 2 mice). Only 10.5% of climbing fibers showed EGFP signal alone

(judged to be "false positive") and 2.1% exhibited mOrange2 signal alone (judged to be

"false negative") (Fig. 5c, green and red blocks, respectively). It should be noted,

however, that, this quantitative analysis may have underestimated the actual percentage

of doble positive climbing fibers because of relatively low expression of mOrange2

compaed to EGFP at this time point (EGFP:mOrange=4:1). This result indicate that

majority of climbing fibers express both proteins when a mixture of two independent

lentiviral vectors for the expression of respective proteins is injected into the inferior

olive. Based on this result, I infected mixture of the lentiviral vector for TNLC

expression and that for EGFP expression to inferior olivary neurons of WT pups at P1

(also see materials and methods).
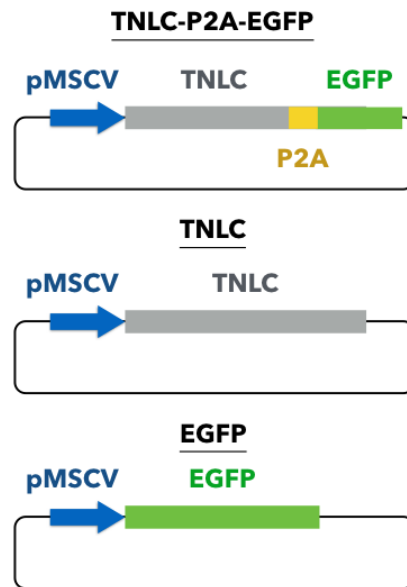
Figure 4. Vectors for expressing TNLC

Cartoons representing the design of three lentiviral vectors modified from the pCL20c-MSCV vector. Colored arrows and rectangles represent sequences as described below: blue arrow: MSCV promoter; green rectangle: EGFP; gray rectangle: sequence coding the TNLC; yellow rectangle: sequence coding the linker containing self-cleaving P2A peptide.
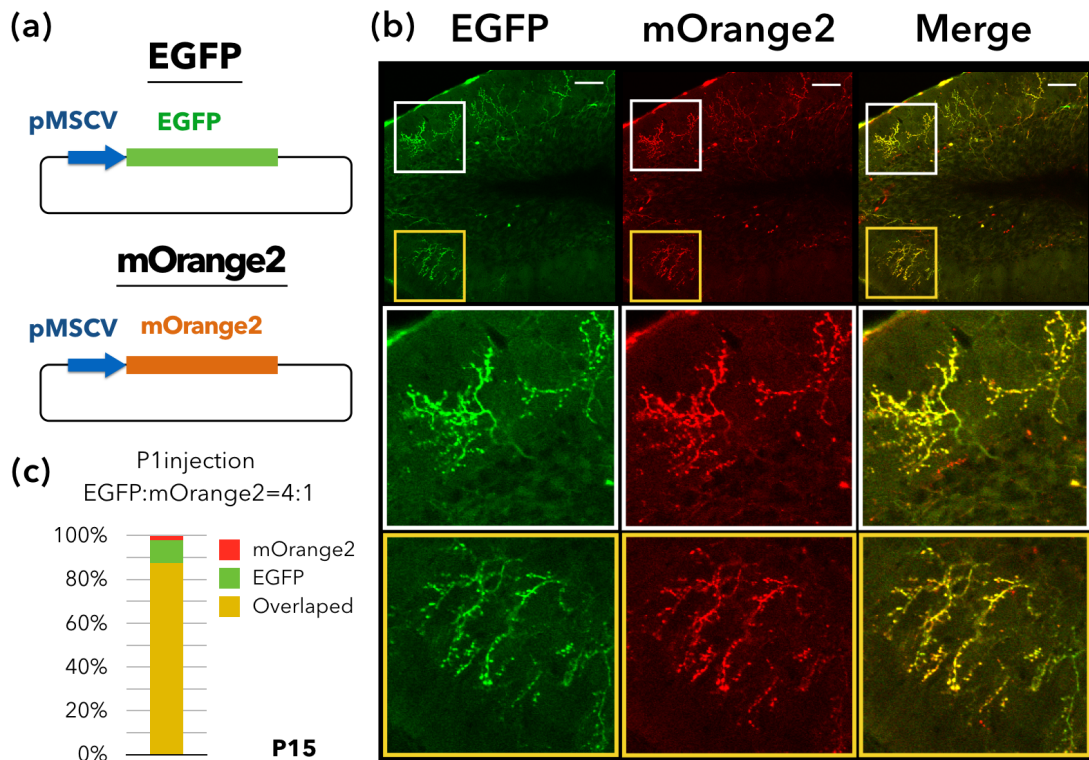
Figure 5. Overlapped expression of EGFP and mOrange2 in climbing fibers by mixture of two lentivirus vectors for transfection of respective constructs.
a. Cartoons representing the design of two lentiviral vectors modified from the pCL20c-MSCV vector. Colored arrows and rectangles represent sequences as described below: blue arrow: MSCV promoter; green rectangle: EGFP; orange rectangle: mOrange2. b. Upper row: Representative image of fixed slices from adult WT mice infected with EGFP+mOrange2 (ratio=1:1). Images representing fluorescent signals of EGFP (green, left), those of mOrange2 (red, middle), and those merged for both (yellow, right). Middle and lower rows: Close-up images of the white (middle) and yellow (lower) rectangular areas of the original images in the upper row. The scale bars represent 80 μm. c. Bar graph showing the co-expression level of EGFP and mOrange2 at P15 (n=237, from two mice). Mice were infected at P1 with a mixture of lentiviral vectors for transfection of EGFP and mOrange2, respectively, at the ratio of 4:1. The yellow, green and red blocks represent EGFP and mOrange2 double positive (overlapped, 87.3%), EGFP single positive- (EGFP, 10.5%) and mOrange2 single positive (mOrange2, 2.1%) climbing fibers, respectively.

I optimized the mixture ratio of the two lentiviral vectors, and found that the TNLC to EGFP ratio of 1 to 4 yielded the best results in terms of the low lethality and the potency of suppression of synaptic transmission. By using this ratio, I investigated the time required to suppress climbing fiber to Purkinje cell synaptic transmission after injection of lentiviral vectors into the inferior olive. To avoid a possible contamination of EPSCs arising from non-infected climbing fiber(s) projecting to the same Purkinje cells, I performed lentiviral infection at P16 (Fig. 6a) when most Purkinje cells are innervated by single climbing fibers (Hashimoto and Kano, 2013). Infections with the optimized mixture (TNLC:EGFP=1:4) resulted in sufficient expression of EGFP in climbing fibers 4 days after the injection of the mixture into the inferior olive at P16 (Fig. 6b). I examined the effect of TNLC on climbing fiber synaptic transmission electrophysiologically after P20 (Day4, Fig 6a). I made whole-cell patch-clamp recordings from Purkinje cells using an internal solution containing fluorescent dye (Alexa568) to confirm that the recorded Purkinje cells were innervated by EGFP positive climbing fibers (Fig. 6b). I found that stimulation of EGFP positive climbing fibers induced no EPSCs in Purkinje cells of mice infected with the mixture of the lentiviruses for the expression of TNLC and EGFP 4 or 5 days after the infection (Fig 7). In marked contrast, stimulation of EGFP positive climbing fibers induced typical large EPSCs in an all-or-none fashion in Purkinje cells of mice infected with the lentivirus for the expression of EGFP alone (Fig. 8). The amplitude of EPSCs elicited by stimulating EGFP positive climbing fibers was the same as that of EPSCs by stimulating EGFP negative climbing fibers (Fig. 8). Thus, these results confirmed that infection of the mixture of lentiviruses for EGFP and TNLC expression into inferior olivary neurons completely abolished glutamate release from climbing fibers expressing EGFP within

days after infection. This method can be used to evaluate the roles of synaptic activity in climbing fiber to Purkinje cell synapse elimination during early postnatal days.

(a)

(b) EGFP / Alexa 568
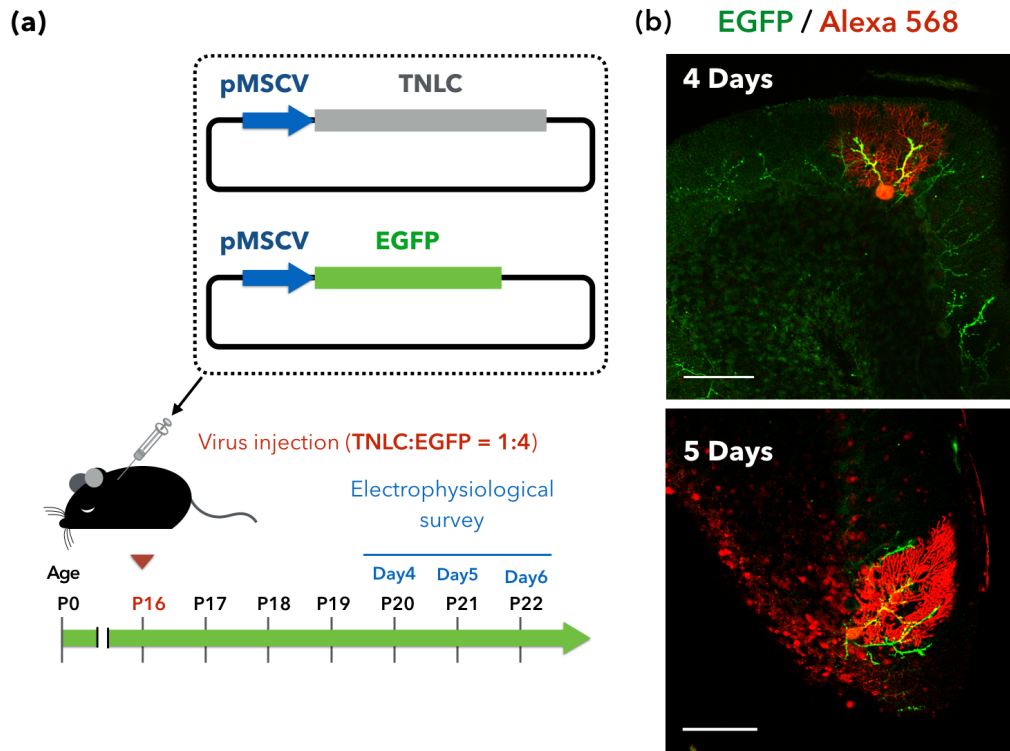
Figure 6. Infection of the lentivirus for TNLC and that for EGFP at the ratio of 1 to 4 into inferior olivary neurons produces sufficient EGFP expression in climbing fibers within 4 days.

a. Timeline for the experimental procedures. Inverted red triangle indicates viral infection at P16. b. Representative confocal images from acute cetrebellar slices right after electrophysiological experiments at 4 (upper) or 5 (lower) days after TNLC + GFP infection into inferior olivary neurons. green, EGFP; red, Alexa 568, red. The scale bars represent 100 μm.

(a)

EGFP + TNLC co-infected mice

Day 4   Day 5

Non-infected | TNLC   Non-infected | TNLC

(b)
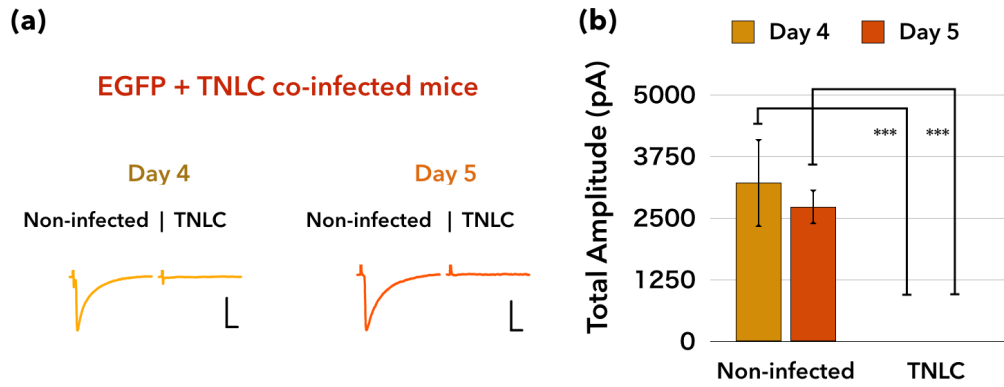
Figure 7. Infection of the lentivirus mixture with the TNLC to EGFP ratio of 1 to 4 completely abolishes climbing fiber to Purkinje cell synaptic transmission within 4 days *in vivo*.

a. Example traces of EPSCs (EPSCs$_{total}$) elicited by stimulating infected (TNLC) or non-infected climbing fiber(s) in Purkinje cells from the infected mice shown in Figure 6. The vertical and horizontal scale bars represent 2 nA and 5 ms. respectively. b. Bar graphs presenting averaged values of EPSCs$_{total}$ elicited by stimulating infected (TNLC) and non-infected climbing fiber(s) in the same slices from mice at 4 days (orange) or 5 days (red) after infection (day 4, n=9, 6; day 5, n=11, 12; for control or TNLC group, respectively). *** $p < 0.001$, n.s. $p > 0.05$ (Wilcoxon–Mann–Whitney test). Error bars stand for ± SEM.

32
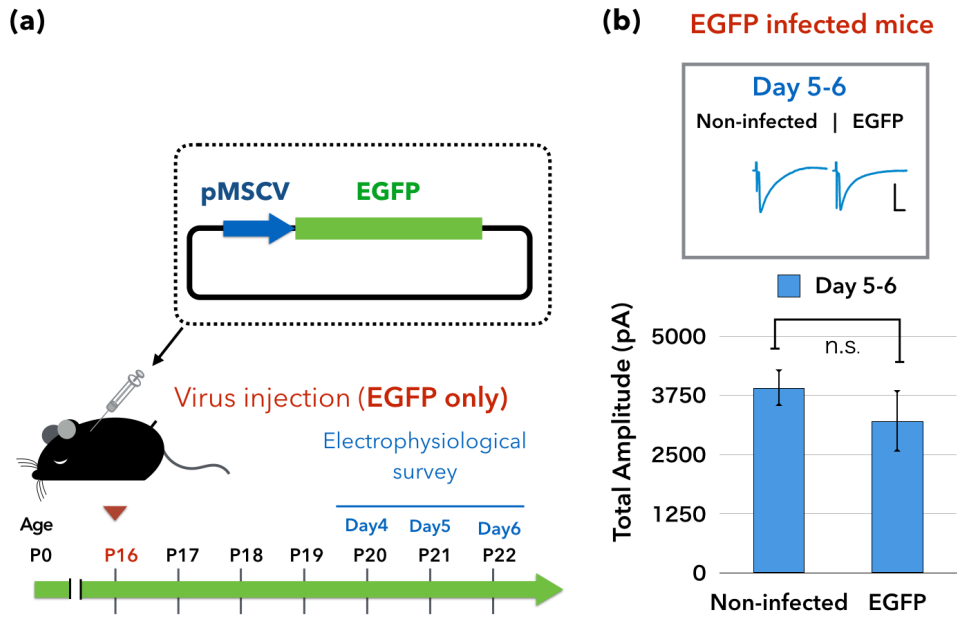
Figure 8. Infection of the lentivirus for EGFP expression into inferior olivary neurons has no effect on climbing fiber to Purkinje cell synaptic transmission.
a. Timeline for the experimental procedures shown similarly to Figure 6. b. Example traces of climbing fiber-mediated EPSCs (upper) and bar graphs (lower) presenting averaged values of EPSCs (EPSCs$_{total}$) elicited by stimulating infected (EGFP) and non-infected (control) climbing fiber(s) in the same slices from mice 5-6 days after infection (n=14 for both control and EGFP groups). The vertical and horizontal scale bars in the box represent 2 nA and 5 ms, respectively. n.s. *p> 0.05* (Wilcoxon–Mann–Whitney test). Error bars stand for ± SEM.

Inactivated climbing fibers incapable of releasing glutamate can become single "winner climbing fibers" but exhibit impaired translocation onto Purkinje cell dendrites

I next tested whether inactive climbing fibers expressing TNLC could translocate onto Purkinje cell dendrites as "winner" climbing fibers (Hashimoto et al., 2009). I performed immunohistochemical analyses in fixed cerebellar slices to visualize climbing fiber synaptic terminals and Purkinje cells by immunolabeling using antibodies against vGluT2 and Car8, respectively. In addition, to visualize a part of control climbing fibers with EGFP, I used a transgenic mouse line in which EGFP is expressed in a subset of inferior olivary neurons under the control of a neurofilament light polypeptide promoter (nefl-EGFP mice) (Carrillo et al., 2013). I injected two lentiviral vectors, one for the expression of TNLC and the other for the expression of mOrange2, into nefl-EGFP mice at P1 to yield a condition in which a subset of Purkinje cells would be innervated by inactive climbing fiber(s) expressing TNLC plus mOrange2 and by active climbing fiber(s) expressing EGFP (Fig. 9a). I found that TNLC-expressing mOrange2-positive climbing fibers clearly translocated onto Purkinje cell dendrites after P20 (Fig. 9b, left). These TNLC-expressing climbing fibers formed vGluT2-positive puncta onto Purkinje cells (Fig. 9b, right) similar to that described in intact climbing fibers. I also noticed that the relative height of the tips of TNLC-expressing climbing fibers was significantly lower than that of non-infected control climbing fibers and that of EGFP-positive control climbing fibers (Fig 9c, control: 66% ± 1.24%; TNLC: 53% ± 2.88%). To check whether the TNLC-expressing climbing fibers were incapable of releasing glutamate at the age of the morphological examination, I made whole-cell recording from Purkinje cells at P18-P24 whose dendrites were occupied by TNLC-infected climbing fibers and stimulated the climbing

fibers. However, I could never evoke any detectible EPSCs (Fig. 9e-g). Collectively, these results indicate that inactive climbing fibers incapable of releasing glutamate can translocate onto Purkinje cell dendrites as "winner" climbing fibers but their dendritic translocation is incomplete compared with that of normal climbing fibers. This moderately impaired dendritic translocation is similar to that of climbing fibers with SNAP25 knockdown, which is shown in the previous section of this thesis.
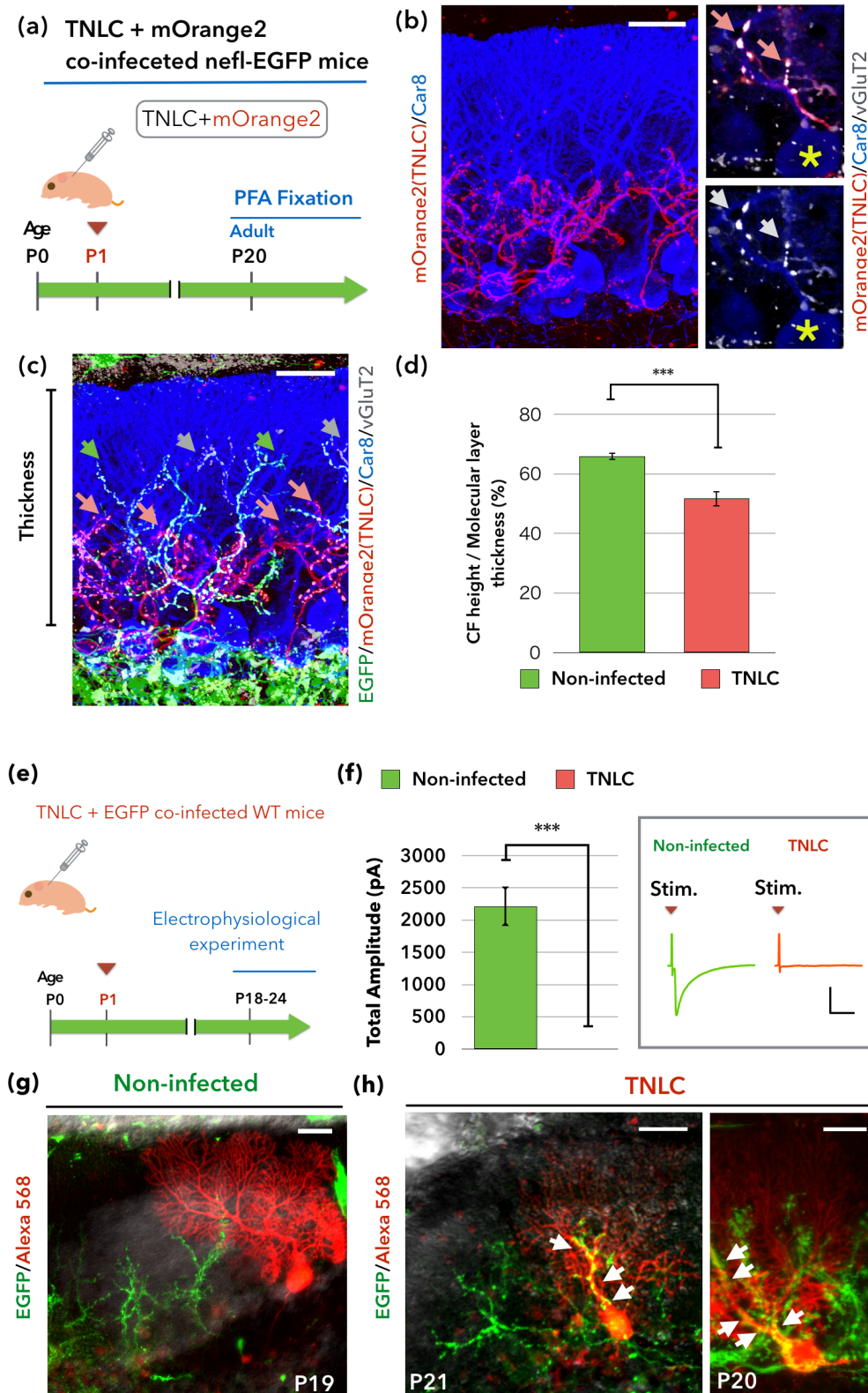
Figure 9. Climbing fibers expressing TNLC can become "winners" but exhibit incomplete translocation to Purkinje cell dendrites.

a. Schedule for immunohistochemical experiments. b. Representative immunolabeled images of infected adult nefl-EGFP mice. Left: merged image for mOrange2 (red) and Car8 (blue) fluorescent signals. Right: close-up images from the left merged for

mOrange2, Car8 and vGluT2 (white) channels (upper) and for Car8 and vGluT2 channels (lower). Arrows emphasize vGluT2-positive puncta on Purkinje cells. Yellow stars indicate the soma of the Purkinje cell. c. The same image as (b) but merged for EGFP (green), mOrange2, Car8, and vGluT2 channels. Arrows emphasize the upmost edge of infected (red) or non-infected control (green or gray) climbing fibers. d. Bar graphs present the climbing fiber height normalized by the thickness of the corresponding molecular layer for infected (red) and non-infected (green) climbing fibers. (TNLC: 53 ± 3%, n= 33; control: 66 ± 1%, n= 47; from 2 mice). *** $p< 0.001$ (t-test). Error bars stand for ± SEM. e. Timeline for the experiments shown in f-h. f. Bar graphs show the averaged $EPSC_{total}$ from Purkinje cells of mice infected at P1 and recorded at P18-24 (for control, n = 16; for TNLC, n= 13; data were collected from 7 mice each). Box in the right present representative traces of EPSCs in Purkinje cells whose dendrite were occupied by a non-infected control climbing fiber (non-infected, green) and by TNLC infected climbing fibers (TNLC, red). g, h. Representative confocal images of acute cerebellar slices of non-infected group (g) and TNLC infected group (h) from P19-21 mice for electrophysiological experiments shown in (f). The fluorescent signals of Alexa 568 and EGFP are shown in red and green, respectively. ** $p< 0.01$ (Wilcoxon–Mann–Whitney test). Error bars stand for ± SEM. The scale bars represent 30 μm.

Severely weakened/inactivated climbing fibers of defective glutamate release compete with normal climbing fibers in early postnatal days.

I next examined whether inactive climbing fibers incapable of releasing glutamate competed with normal climbing fibers during the processes of climbing fiber synapse elimination. I performed immunohistochemical analyses in juvenile nefl-EGFP mice at P8 that had been infected with the mixture of the lentiviral vector for TNLC expression and that for mOrange2 expression. I found that Purkinje cells innervated by TNLC-infected climbing fibers (mOrange2-positive) were innervated also by non-infected climbing fibers (presented as EGFP-positive puncta or EGFP-negative vGluT2-positive puncta) on their somata (Fig. 10). These data clearly show that inactive climbing fibers incapable of releasing glutamate project to Purkinje cells that are innervated by normal climbing fibers during postnatal development. To substantiate this possibility, I performed electrophysiological analyses of the developing mice that had been infected with the viral mixture at P1 (Fig. 11a). I made whole-cell patch-clamp recording from Purkinje cells at P5 and P8 using an internal solution containing fluorescent dye (Alexa568). Under the fluorescent microscope attached to.the patch-clamp set-up, I checked the distribution of TNLC-expressing climbing fibers in cerebellar slices. After whole-cell recording, Purkinje cells contacted by infected climbing fibers were assigned to TNLC group (Fig. 11b) and those innervated by non-infected normal climbing fibers were assigned to the control group. Purkinje cells in the TNLC group showed markedly decreased $EPSC_{total}$ compared to those in the control group (Fig. 11c). Moreover, I found that over ~50% of Purkinje cells in the TNLC group had small but clearly detectable $EPSC_{total}$ (the portion of Purkinje cells with detectable EPSCs: control, 89% at P5 and 100% at P8; TNLC, 47% at P5 and 72% at P8), although the others showed no detectable $EPSC_{total}$ (Fig. 11d). In this experiment,

some Purkinje cells had no detectable climbing fiber-driven EPSCs in the TNLC group at P5 (the 4th day after viral infection at P1). This result indicates that TNLC-infected climbing fibers projecting to these Purkinje cells were totally incapable of releasing glutamate at P5. Such Purkinje cells account for 53% in the TNLC group, whereas only 11% of Purkinje cells showed no response in the control group at the same age. As to the rest of Purkinje cells (47%) in the TNLC group at P5, EPSCs with very small amplitudes were elicited (Fig. 11d). These tiny EPSCs might represent activity of climbing fibers with partially impaired glutamate release by TNLC expression. However, I assume this possibility is unlikely because transfection of TNLC into the inferior olive at P16 with the same method used at P1 completely abolished glutamate release from infected climbing fiber at P20 i.e., 4 days after TNLC infection (Fig. 7). An alternative possibility is that the tiny EPSCs arose from non-infected intact climbing fibers that co-innervated the recorded Purkinje cells with TNLC expressing dominant climbing fibers. If the tiny EPSCs were caused by non-infected climbing fibers, it indicates that nearly 50% of Purkinje cells innervated by TNLC-expressing inactive climbing fibers were also innervated by non-infected intact climbing fibers at P5 and P8. Collectively, these lines of evidence suggest that climbing fibers with severely impaired/inactivated glutamate release compete with normal climbing fibers for Purkinje cell innervation at P5 and thereafter.

TNLC + mOrange2 co-infected nefl-EGFP mice

EGFP/mOrange2/Car8/vGluT2
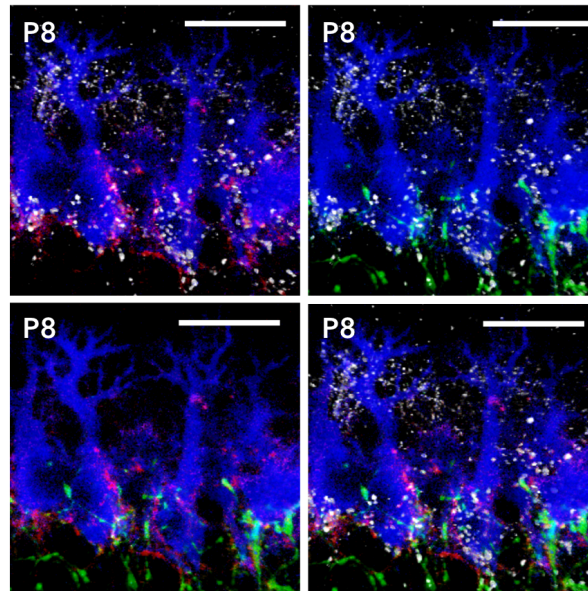
Figure 10. Morphological evidence for Purkinje cells co-innervated by inactive climbing fibers incapable of releasing glutamate and normal climbing fibers at P8. Example confocal images from a nefl-EGFP mouse at P8 that was infected with TNLC + mOrange at P1. Artificial colors assigned to EGFP, mOrange2, Car8 and vGluT2 are green, red, blue, and gray, respectively. Different activated channels for the images are: EGFP + vGluT2 + Car8 (upper left); mOrange2 + vGluT2 + Car8 (upper right); EGFP + mOrange2 + Car8 (lower left); EGFP + mOrange2 + vGluT2 + Car8 (lower right). The scale bars represent 30 μm.
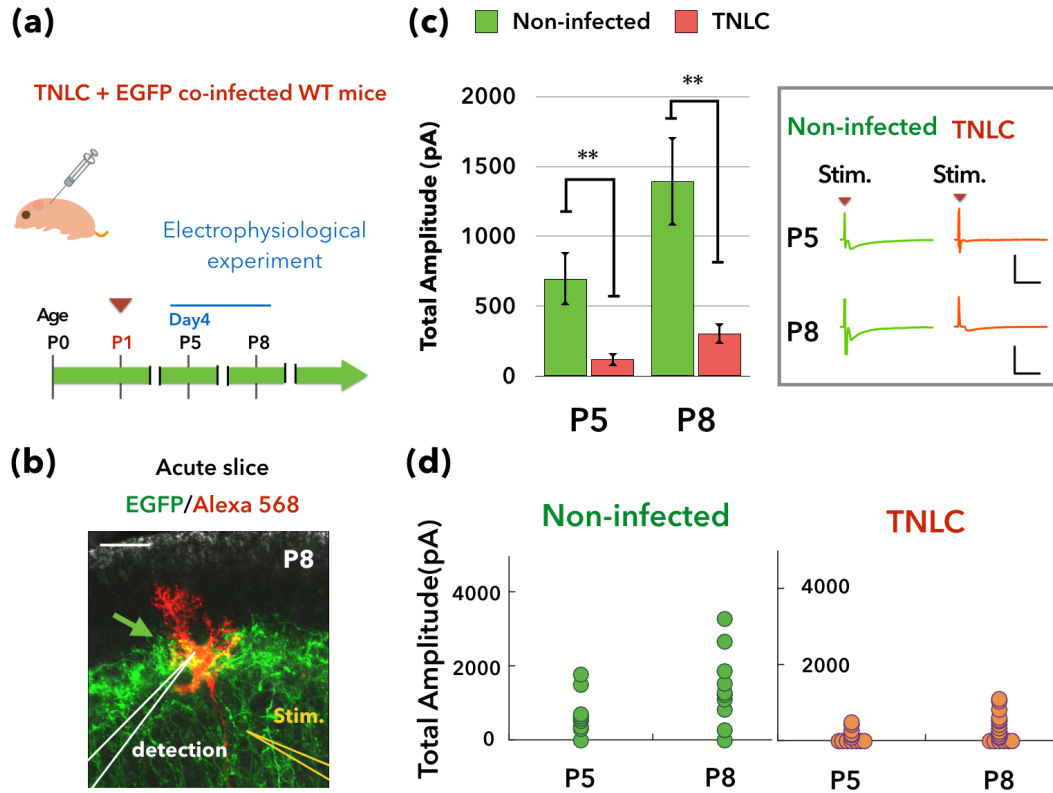
Figure 11. Functional evidence for the competition between inactive climbing fibers incapable of releasing glutamate and normal climbing fibers at P5 and P8.
a. Timeline for the experimental procedures. b. Representative confocal image of an acute cerebellar slice from a P8 mouse for obtaining the data shown in (c, d). The fluorescent signals of Alexa 568 and EGFP are shown in red and green, respectively. The green arrow emphasizes the contact of infected climbing fiber(s) to the recorded Purkinje cell. Configurations of recording and stimulation electrodes are shown over the fluorescent image. The scale bars represent 30 μm. c. (left) Bar graphs showing the averaged $EPSC_{total}$ from P5 and P8 (for non-infected control, n = 9 (P5), n = 10 (P8); for TNLC, n= 13 (P5), 21 (P8); data were collected from 4 and 5 mice for P5 and P8 respectively). (right) Representative traces of EPSCs in Purkinje cells at P5 (upper) and P8 (lower) elicited by stimulating uninfected control climbing fibers (non-infected control, green) and stimulation in areas where infected climbing fibers (TNLC, red). The vertical and horizontal scale bars represent 2 nA and 5 ms, respectively. d. Dotted plots representing the distribution of raw $EPSC_{total}$ data from individual Purkinje cells elicited by stimulating non-infected control (upper, closed circles in green) and infected (below, closed circles in red) climbing fiber(s). Circles corresponding to 0 pA were lined. ** $p< 0.01$ (Wilcoxon–Mann–Whitney test). Error bars stand for ± SEM.

Climbing fiber to Purkinje cell synaptic strength is not required for the ultimate winner-loser selection.

Next I examined whether climbing fiber to Purkinje cell synaptic transmission is essential for ultimate determination of the winner and loser climbing fibers, I calculated the proportion of Purkinje cells innervated by TNLC-expressing climbing fibers on the dendrites as single winners among the Purkinje cells innervated by both infected and non-infected climbing fibers. I injected a mixture of lentivirus for EGFP expression and that for TNLC expression at P1, or only lentivirus for EGFP expression at P1. I noticed that dendritic translocation of TNLC-expressing climbing fibers was retarded by about 3 days when compared to that of control climbing fibers (Fig. 12a). Therefore, for comparison of climbing fiber innervation patterns, I used mice at P15 for climbing fibers expressing TNLC plus EGFP and mice at P12 for climbing fibers expressing EGFP alone. I analyzed Purkinje cells that were clearly occupied by both EGFP positive climbing fibers and negative climbing fibers. I found that the proportion of climbing fibers that became winners was nearly the same between climbing fibers expressing TNLC plus EGFP and those expressing EGFP alone. (Fig. 12b, c). This result suggests that certain proportion of climbing fibers ultimately become winners with severely weakened/inactivated synaptic activity they elicit in Purkinje cells.
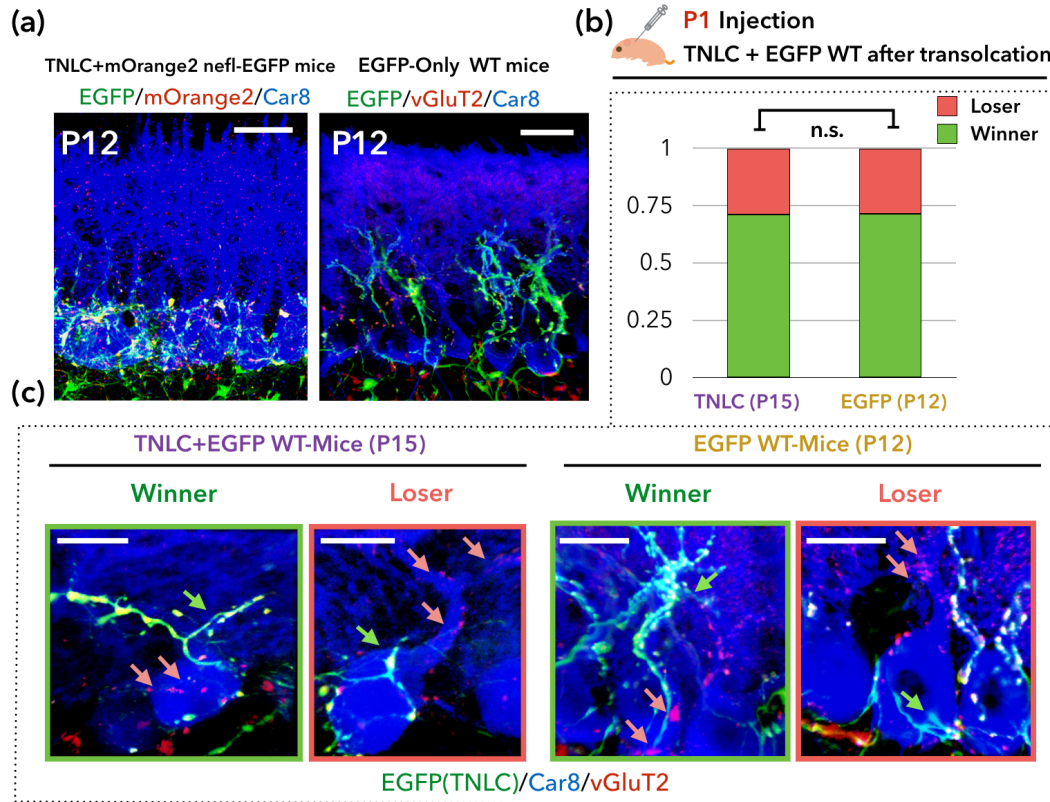
Figure 12. Ablation of climbing fiber to Purkinje cell synaptic transmission has no impact on the ultimate selection of winners and losers.

a. (Left) Representative images from P12 cerebellum of nefl-EGFP mice infected with TNLC + mOrange2 showing delayed climbing fiber translocation. Artificial colors represent fluorescent signals of EGFP (green), mOrange2 (red) and Car8 (blue). Signals from the vGluT2 channel are omitted in this figure for simplicity. (Right). Representative image from P12 cerebellum of mice infected with lentivirus for EGFP expression showing normal climbing fiber translocation. Artificial colors represent fluorescent signals of EGFP (green), mOrange2 (red) and Car8 (blue). The scale bars in (a) represent 30 μm. b. Bar graph showing the proportion of winners (green) and losers (red) among EGFP-positive climbing fibers in mice infected with TNLC + EGFP (left column, n= 52 climbing fibers from 2 mice at P15) and those infected with EGFP alone (right column, n= 56 climbing fibers, from 2 mice at P12). There is no significant difference between TNLC+EGFP infected mice and EGFP infected mice. n.s. *p> 0.05* (ChiSquare-Test). c. Example images of Purkinje cells with an infected climbing fiber as winner (left panel) or loser (right panel). Artificial colors represent fluorescent signals of EGFP (green), Car8 (blue), and vGluT2 (red). Colored arrows emphasize vGluT2 puncta that are positive (green) or negative (red) for EGFP of infected climbing fibers. The scale bars in (c) represent 20 μm.

Severe impairment of elimination of redundant climbing fiber synapses in Purkinje cells with single winner climbing fibers incapable of releasing glutamate

Finally, I examined whether elimination of redundant climbing fiber synapses was impaired in Purkinje cells whose dendrites are occupied by single inactive climbing fibers incapable of releasing glutamate as "winners". I looked for Purkinje cells whose dendrites were innervated by single winner climbing fibers expressing EGFP or mOrange2. If the somata of such Purkinje cells were contacted by vGluT2-positive puncta without EGFP or mOrange2, they were judged to be multiply-innervated by climbing fibers with different origins in the inferior olive (Mikuni et al., 2013; Kawata et al., 2014; Uesaka et al., 2014). I found that about 20% of Purkinje cells that had fluorescent protein positive winner climbing fibers on their dendrites showed multiple innervation in wild-type and control nefl-EGFP mice which had been infected with lentiviral vectors for expression of fluorescent protein (EGFP for WT and mOrange for nefl-EGFP mice) (Fig. 13a). These results for control mice were similar to those of the previous studies (Nakayama et al., 2012; Mikuni et al., 2013; Kawata et al., 2014). By marked contrast, about 80% of Purkinje cells in which single TNLC-expressing climbing fibers translocated onto their dendrites had clearly redundant climbing fiber synapses on their somata in nefl-EGFP mice which had been infected with lentiviral vectors for the expression of TNLC and mOrange (Fig. 13a). These results are consistent with those of the previous stiudies (Hashimoto et al., 2011; Kawamura et al., 2013; Mikuni et al., 2013; Kawata et al., 2014), and support the notion that elimination of redundant climbing fiber synapses depends heavily on synaptic inputs from climbing fibers to Purkinje cells and subsequent activation of P/Q-type voltage-dependent Ca^{2+} channels, Ca^{2+} influx into Purkinje cells, and activation of *Arc*.
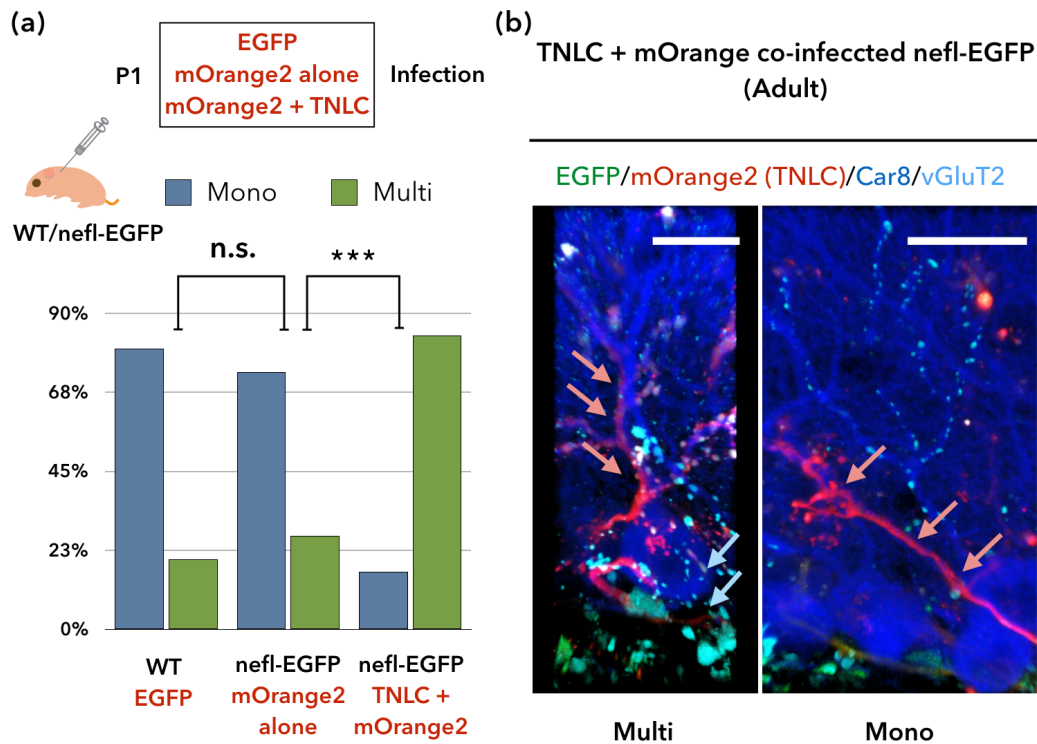
Figure 13. Impaired elimination of redundant climbing fiber synapses from the soma in Purkinje cells with single winner climbing fibers incapable of releasing glutamate

a. Bar graph presenting the percentage of analyzed Purkinje cells innervated by one or multiple climbing fiber(s) in adult wild-type mice transfected with EGFP, adult nefl-EGFP mice transfected with mOrange2 (nefl-EGFP control), and adult nefl-EGFP mice transfected with TNLC plus mOrange2 (nefl-EGFP TNLC). Percentage of mono-innovation for each group is as follows. WT: 80%, n= 63, from two P34 mice; nefl-EGFP control: 73%, n= 60, from two P24 mice; nefl-EGFP TNLC: 16 %, n= 55, from P22 and P44 mice. *** $p < 0.001$, n.s. $p > 0.05$ (ChiSquare-Test). b. Example images presenting analyzed Purkinje cells with multiple climbing fiber innervation (left) and mono climbing fiber innervation (right) after maturation. Artificial colors assigned to each channel are EGFP: (green), mOrange2 (red), Car8 (blue), and vGluT2 (cyan). Colored arrows emphasize climbing fibers expressing TNLC (red) and vGluT2 puncta without mOrange2 fluorescence (cyan) that have different origins in the inferior olive from TNLC-expressing climbing fibers. The scale bars represent 20 μm and 30 μm in the pictures representing a multi (left) and a mono (right) Purkinje cells, respectively.

CONCLUSIONS AND DISCUSSIONS

In this thesis, I have disclosed an unexpected nature of developmental synapse elimination in the cerebellum that the selection of a winner and losers occurs in a manner independent on synaptic strength. It has been generally thought that stronger synapses will be further strengthened and stabilized depending on the stregth of synaptic input in many regions of developing nervous system including the neuromuscular junction, hippocampus, retino-geniculate synapse, visual cortex and somatosensory cortex. In the cerebellum, it has also been believed that synaptic activity is essential for the selection of winner and loser climbing fibers, dendritic translocation of a single winner climbing fiber, and elimination of redundant loser climbing fibers. A recent time-lapse imaging study demonstrated that once-losing climbing fibers could translocate to vacant dendrite of Purkinje cell when the winning climging fiber was laser-ablated at P11-P12 (Carrillo et al., 2013), suggesting that the winner climbing fiber can be replaced by another one even after the winner is determined. It is possible that once-losing climbing fibers may change their properties after the ablation of the competing winner climbing fiber. Alternatively, there may be "ranking" among multiple climbing fibers innervating individual Purkinje cells. When the climbing fiber of the first rank is ablated, the one of the second rank may become the winner.

In a previous study from our laboratory, Hashimoto et al. demonstrated a severe defect in functional differentiation of immature climbing fibers in Purkinje cell-specific P/Q-type voltage-dependent Ca^{2+} channel knockout mice (Hashimoto et al., 2011). Systematic electrophysiological investigation in cerebellar slices at P3 to P8 revealed that the biased strengthening of single climbing fibers was severely impaired in Purkinje cells lacking P/Q-type voltage-dependent Ca^{2+} channel (Hashimoto et al., 2011). Furthermore, a subsequent *in vivo* electrophysiological study by Kawamura et al.

confirmed the impaired biased strengthening of single climbing fibers in P/Q-type voltage-dependent Ca^{2+} channel knockout Purkinje cells (Kawamura et al., 2013). In acute cerebellar slices at P6-P8, stimulation of "stronger" climbing fiber inputs in conjunction with depolarization of Purkinje cell caused LTP, whereas stimulation of "weaker" climbing fiber together with Purkinje cell depolarization led to LTD (Bosman et al., 2008; Ohtsuki and Hirano, 2008). These lines of evidence support that single winner climbing fibers are established in individual Purkinje cells in an activity dependent manner and Ca^{2+} influx into Purkinje cells through P/Q-type voltage-dependent Ca^{2+} channel is crucial for the process. This notion is in line with the aforementioned "ranking" hypothesis and suggests the possibility that the "rank" of an individual climbing fiber in dendritic translocation might be determined by their order in synaptic strength. However, in the present study, I found that climbing fibers expressing TNLC (infected at P1) had an ability to become a subsequent "winner" climbing fiber. In my electrophysiological experiment using mice infected at P1, I observed a severely impaired/inactivated glutamate release from TNLC-infected climbing fibers at P5 and thereafter. Despite almost complete blockade of glutamate release, my morphologocal data clearly suggest that certain portions of TNLC-infected inactive climbing fibers ultimately become winners at P15 by beating non-infected intact climbing fibers. These results collectively indicate that, at least after P5, climbing fiber synaptic activity contributes little, if any, to the establishment of a single winner climbing fiber in each Purkinje cell. This unexpected result also indicates that the rank order of multiple climbing fibers, if it is present, is independent of strengths of synaptic inputs. At present, it is unknown how the strongest climbing fiber undergo dendritic translocation without synaptic activity.

It should be noted that in Purkinje cell-specific P/Q-type voltage-dependent Ca^{2+} channel knockout mice, selective strengthening of single climbing fiber inputs (functional differentiation) is severely impaired from P5 to P8 but the difference in synaptic strength becomes gradually larger from P8 and thereafter (Hashimoto et al., 2011). At P17, single climbing fiber inputs are more than twice stronger than the rest of climbing fiber inputs in individual Purkinje cells of P/Q-type voltage-dependent Ca^{2+} channel knockout mice (Hashimnoto et al., 2011), indicating that functional differentiation is significantly delayed but is not completely defective in Purkinje cells lacking P/Q channels. Thus, instead of participating in the selection of a solo "winner" climbing fiber to each Purkinje cell, P/Q-type voltage-dependent Ca^{2+} channels in Purkinje cell are considered to play mandatory roles in the strengthening of a single climbing fiber that is presumably predetermined to win during the proper timing of postnatal development.

The present study demonstrate a moderately reduced dendritic translocation of winner climbing fibers that are incapable of releasing glutamate (Fig. 9), which is in agreement with the results of the previous studies on mice that have reduced climbing fiber synaptic inputs (Kawata et al., 2014) or climbing fiber-mediated Ca^{2+} transients in Purkinje cells through P/Q-type voltage-dependent Ca^{2+} channels (Hashimoto et al., 2011). These results clearly indicate that climbing fiber to Purkinje cell synaptic transmission is necessary for proper expansion of a single winner climbing fiber along Purkinje cell dendrites and completion of its translocation, persumably through mechnisms involving P/Q-type voltage-dependent Ca^{2+} channels.

This study also has proved that synaptic inputs from a single winner climbing fiber are essential for the elimination of somatic synapses of the loser climbing fibers. This data is consistent with the results of the previous studies on mice that have reduced

climbing fiber synaptic inputs (Kawata et al., 2014). However, it was unclear whether synaptic inputs from a winner climbing fiber or those from loser climbing fibers are important for the elimination of loser climbing fiber synapses. I have found that redundant climbing fiber synapses that normally release glutamate remain on the somata of Purkinje cells innervated by single winner climbing fibers that cannot release glutamate (Fig. 9f, Fig. 13). This result clearly indicates that synaptic inputs from winner climbing fibers to individual Purkinje cells are essential for the elimination of redundant climbing fiber synapses on the somata. This impairment is likely to result from the lack of Ca^{2+} transients in Purkinje cells through P/Q-type voltage-dependent Ca^{2+} channels and subsequent activation of the immediate early gene *Arc/Arg3.1* (Hashimoto et al., 2011; Mikuni et al., 2013).

The present study does not completely elucidate the timing when one climbing fiber is selected as a winner. One possible mechanism is that a single winner climbing fiber is already determined before its translocation to Purkinje cell dendrites. It is possible that synaptic inputs before P5 is enough to determines a single climbing that becomes the winner thereafter. Alternatively, the future winner climbing fiber is predetermined at the time of birth although multiple climbing fibers have similar strengths at birth and the future winner cannot be distinglushed.

Mechanisms for the discrimination of a single winner climbing fiber still remain unknown. One possibility is that a single climbing fiber that innervates each Purkinje cell throughout life is predetermined, that is, a single winner climbing fiber is not selected through competition of multiple climbing fibers with equal opportunities to win. The present study does not elucidate possible signaling molecules that are independent of climbing fiber synaptic activity but are involved in the determination of a single winner climbing fiber. A previous study on the NMJs using culture preparations

suggests that proBDNF weakens synaptic connections of axons with less neuronal activity through axonal p75 receptor. This study also suggests that BDNF generated from proBDNF by a protease derived from presynaptic terminals stabilizes synaptic connections of the more active axon through axonal TrkB receptor (Je et al., 2012). Furthermore, it has recently been found that semaphorins function as retrograde signaling molecules to influence processes of climbing fiber synapse elimination (Uesaka et al., 2014). By analogy with this result, it is likely that retrograde signaling molecules may plays a role in the discrimination of winner and loser climbing fibers. Another possible mechanism is presynaptic tagging of climbing fiber terminals by molecules which trigger subsequent events mediated by microglia. Studies in the retino-geniculate synapses suggest that the tagging of synapses by an immune-related molecule, C1q, regulates synapse elimination and triggers engulfment of less active synapses by microglia (Stevens et al., 2007; Bialas and Stevens, 2013). A recent study on the cerebellum demonstrates the involvement of an immune-relative molecule, C1ql1, in the strengthening and maintenance of a single winner climbing fiber. However, this study also showed that disparity among multiple climbing fiber inputs was normal and a single climbing fiber translocated onto the dendrite of each Purkinj cell in C1ql1 knockout mice (Kakegawa et al., 2015). It is therefore useful to search candidate molecules involved in the selection of a single winner climbing fiber from retrograde signaling and immune molecules by using the methods adopted for the identification of semaphorins as retrograde signaling molecules for climbing fiber synapse elimination (Uesaka et al., 2014). The results from these experiments may further deepen our knowledge about how a single winner climbing fiber is selected in each Purkinje cell in the developing cerebellum.

Taken together, the present study have disclosed the roles of synaptic activity in the processes of climbing fiber synapse elimination in the developing cerebellum, and gives a new insight into the mechanisms of neural circuit refinement in the developing nervous system.

AKNOWLEDGEMENTS

REFERENCES

Aiba A, Kano M, Chen C, Stanton ME, Fox GD, Herrup K, Zwingman TA, Tonegawa S (1994) Deficient cerebellar long-term depression and impaired motor learning in mGluR1 mutant mice. Cell 79:377–388.

Bialas AR, Stevens B (2013) TGF-β signaling regulates neuronal C1q expression and developmental synaptic refinement. Nat Neurosci 16:1773–1782.

Blasi J, Chapman ER, Link E, Binz T, Yamasaki S, Camilli PD, Südhof TC, Niemann H, Jahn R (1993) Botulinum neurotoxin A selectively cleaves the synaptic protein SNAP-25. Nature 365:160–163.

Bosman LWJ, Takechi H, Hartmann J, Eilers J, Konnerth A (2008) Homosynaptic Long-Term Synaptic Potentiation of the "Winner" Climbing Fiber Synapse in Developing Purkinje Cells. J Neurosci 28:798–807.

Buffelli M, Burgess RW, Feng G, Lobe CG, Lichtman JW, Sanes JR (2003) Genetic evidence that relative synaptic efficacy biases the outcome of synaptic competition. Nature 424:430–434.

Carrillo J, Nishiyama N, Nishiyama H (2013) Dendritic translocation establishes the winner in cerebellar climbing fiber synapse elimination. J Neurosci 33:7641–7653.

Colman H, Nabekura J, Lichtman JW (1997) Alterations in synaptic strength preceding axon withdrawal. Science 275:356–361.

Crepel FF, Mariani JJ, Delhaye-Bouchaud NN (1976) Evidence for a multiple innervation of Purkinje cells by climbing fibers in the immature rat cerebellum. J Neurobiol 7:567–578.

Godement P, Salaün J, Imbert M (1984) Prenatal and postnatal development of retinogeniculate and retinocollicular projections in the mouse. J Comp Neurol 230:552–575.

Hashimoto K, Ichikawa R, Kitamura K, Watanabe M, Kano M (2009) Translocation of a "winner" climbing fiber to the Purkinje cell dendrite and subsequent elimination of "losers" from the soma in developing cerebellum. Neuron 63:106–118.

Hashimoto K, Kano M (2003) Functional Differentiation of Multiple Climbing Fiber Inputs during Synapse Elimination in the Developing Cerebellum. Neuron 38:785–796.

Hashimoto K, Kano M (2013) Synapse elimination in the developing cerebellum. Cell Mol Life Sci 70:1–14.

Hashimoto K, Tsujita M, Miyazaki T, Kitamura K, Yamazaki M, Shin H-S, Watanabe M, Sakimura K, Kano M (2011) Postsynaptic P/Q-type Ca^{2+} channel in Purkinje cell mediates synaptic competition and elimination in developing cerebellum. Proc Natl Acad Sci USA 108:9987–9992.

Hayakawa I, Kawasaki H (2010) Rearrangement of Retinogeniculate Projection Patterns after Eye-Specific Segregation in Mice Manzoni OJ, ed. PLoS ONE 5:e11001.

Hubel DH, Wiesel TN (1970) The period of susceptibility to the physiological effects of unilateral eye closure in kittens. J Physiol 206:419–436.

Hubel DH, Wiesel TN (1977) Ferrier Lecture: Functional Architecture of Macaque Monkey Visual Cortex. Proc R Soc Lond B Biol Sci 198:1–59.

Je HS, Yang F, Ji Y, Nagappan G, Hempstead BL, Lu B (2012) Role of pro-brain-derived neurotrophic factor (proBDNF) to mature BDNF conversion in activity-dependent competition at developing neuromuscular synapses. Proc Natl Acad Sci USA 109:15924–15929.

Kakegawa W, Mitakidis N, Miura E, Abe M, Matsuda K, Takeo YH, Kohda K, Motohashi J, Takahashi A, Nagao S, Muramatsu S-I, Watanabe M, Sakimura K, Aricescu AR, Yuzaki M (2015) Anterograde C1ql1 signaling is required in order to determine and maintain a single-winner climbing fiber in the mouse cerebellum. Neuron 85:316–329.

Kano M, Hashimoto K (2009) Synapse elimination in the central nervous system. Curr Opin Neurol 19:154–161.

Kawamura Y, Nakayama H, Hashimoto K, Sakimura K, Kitamura K, Kano M (2013) Spike timing-dependent selective strengthening of single climbing fibre inputs to Purkinje cells during cerebellar development. Nat Commun 4:2732.

Kawata S, Miyazaki T, Yamazaki M, Mikuni T, Yamasaki M, Hashimoto K, Watanabe M, Sakimura K, Kano M (2014) Global Scaling Down of Excitatory Postsynaptic Responses in Cerebellar Purkinje Cells Impairs Developmental Synapse Elimination. Cell Rep 8:1119–1129.

Kerschensteiner D, Morgan JL, Parker ED, Lewis RM, Wong ROL (2009) Neurotransmission selectively regulates synapse formation in parallel circuits in vivo. Nature 460:1016–1020.

Lichtman JW, Colman H (2000) Synapse elimination review and indelible memory. Neuron 25:269–278.

Linden DC, Guillery RW, Cucchiaro J (1981) The dorsal lateral geniculate nucleus of the normal ferret and its postnatal development. J Comp Neurol 203:189–211.

Mikuni T, Uesaka N, Okuno H, Hirai H, Deisseroth K, Bito H, Kano M (2013) Arc/Arg3.1 Is a Postsynaptic Mediator of Activity-Dependent Synapse Elimination in the Developing Cerebellum. Neuron 78:1024–1035.

Miyazaki T, Watanabe M (2010) Development of an anatomical technique for visualizing the mode of climbing fiber innervation in Purkinje cells and its application to mutant mice lacking GluRδ2 and Cav2.1. Anat Sci Int 86:10–18.

Nakayama H, Miyazaki T, Kitamura K, Hashimoto K, Yanagawa Y, Obata K, Sakimura K, Watanabe M, Kano M (2012) GABAergic inhibition regulates developmental synapse elimination in the cerebellum. Neuron 74:384–396.

Ohtsuki G, Hirano T (2008) Bidirectional plasticity at developing climbing fiber-Purkinje neuron synapses. Eur J Neurosci 28:2393–2400.

Purves D, Lichtman JW (1980) Elimination of synapses in the developing nervous system. Science 210:153–157.

Schiavo G, Benfenati F, Poulain B, Rossetto O, Polverino de Laureto P, DasGupta BR, Montecucco C (1992) Tetanus and botulinum-B neurotoxins block neurotransmitter release by proteolytic cleavage of synaptobrevin. Nature 359:832–835.

Shatz CJ (1983) The prenatal development of the cat's retinogeniculate pathway. J Neurosci 3:482–499.

Sotelo C, Llinas R, Baker R (1974) Structural study of inferior olivary nucleus of the cat: morphological correlates of electrotonic coupling. J Neurophysiol 37:541–559.

Sretavan DW, Shatz CJ (1986) Prenatal development of retinal ganglion cell axons: segregation into eye-specific layers within the cat's lateral geniculate nucleus. J Neurosci 6:234–251.

Stellwagen D, Shatz CJ (2002) An Instructive Role for Retinal Waves in the Development of Retinogeniculate Connectivity. Neuron 33:357–367.

Stevens B et al. (2007) The classical complement cascade mediates CNS synapse elimination. Cell 131:1164–1178.

Turney SG, Lichtman JW (2012) Reversing the outcome of synapse elimination at developing neuromuscular junctions in vivo: evidence for synaptic competition and its mechanism. PLoS Biol 10:e1001352.

Uesaka N, Uchigashima M, Mikuni T, Nakazawa T, Nakao H, Hirai H, Aiba A, Watanabe M, Kano M (2014) Retrograde semaphorin signaling regulates synapse elimination in the developing mouse brain. Science 344:1020–1023.

Washbourne P, Thompson PM, Carta M, Costa ET, Mathews JR, Lopez-Benditó G, Molnár Z, Becher MW, Valenzuela CF, Partridge LD, Wilson MC (2002) Genetic ablation of the t-SNARE SNAP-25 distinguishes mechanisms of neuroexocytosis. Nat Neurosci 5:19–26.

Watanabe M, Kano M (2011) Climbing fiber synapse elimination in cerebellar Purkinje cells. Eur J Neurosci 34:1697–1710.

Wiesel TN, Hubel DH (1963) Single-cell responses in striate cortex of kittens deprived of vision in one eye. J Neurophysiol 26:1003–1017.

Yasuda M, Johnson-Venkatesh EM, Zhang H, Parent JM, Sutton MA, Umemori H (2011) Multiple forms of activity-dependent competition refine hippocampal circuits in vivo. Neuron 70:1128–1142.

Zhang J, Ackman JB, Xu H-P, Crair MC (2011) Visual map development depends on the temporal pattern of binocular activity in mice. Nat Neurosci 15:298–307.